



## Impedance spectroscopy studies on lead free $(\text{Ba}_{0.85}\text{Ca}_{0.15})(\text{Ti}_{0.9}\text{Zr}_{0.1})\text{O}_3$ ceramics

Ahcène Chaouchi\*, Sadia Kennour

Laboratoire de Chimie Appliquée et Génie Chimique de l'Université Mouloud Mammeri de Tizi-Ouzou, Algeria

Received 20 September 2012; received in revised form 27 November 2012; accepted 3 December 2012

### Abstract

The AC complex impedance spectroscopy technique has been used to obtain the electrical parameters of polycrystalline sample of  $(\text{Ba}_{0.85}\text{Ca}_{0.15})(\text{Ti}_{0.9}\text{Zr}_{0.1})\text{O}_3$  in a wide frequency range at different temperatures. This sample was prepared by a high temperature solid-state reaction technique and single phase formation was confirmed by X-ray diffraction technique. This study was carried out by the means of simultaneous analysis of impedance, modulus, and electrical conductivity. The Cole-Cole (Nyquist) plots suggest that the grains and grain boundaries are responsible in the conduction mechanism of the material at high temperature. The Cole-Cole (Nyquist) plot studies revealed the presence of grain and grain boundary effect at 485 °C. On the other hand, it showed only the presence of grain boundary component of the resistivity at 535 °C. Complex impedance analysis indicated the presence of non-Debye type dielectric relaxation. The bulk resistance of the material decreases with rise in temperature similar to a semiconductor, and the Cole-Cole (Nyquist) plot showed the negative temperature coefficient of resistance (NTCR) character of  $(\text{Ba}_{0.85}\text{Ca}_{0.15})(\text{Ti}_{0.9}\text{Zr}_{0.1})\text{O}_3$ . The value of activation energy is found to be 0.7433 eV, which suggests that the conduction may be the result of defect and charge carriers present in the materials.

**Keywords:**  $\text{BaTiO}_3$  based ceramics, impedance spectroscopy, dielectric relaxation, conductivity

### I. Introduction

Ferroelectric materials with perovskite structures have received much attention due to their excellent functional properties, such as piezoelectricity, pyroelectricity and electrooptic effects, useful for microelectronic devices. Lead-based piezoelectric ceramics have been an industry standard for many decades and are widely used in actuators, sensors, and transducers because of their excellent electrical properties [1]. However, there is growing environmental concern about the use of lead in such products and the European Union has already introduced legislation to restrict the use of a range of hazardous substances which is directly relevant to the piezoelectrics [2].

The newly discovered lead-free  $(\text{Ba,Ca})(\text{Ti,Zr})\text{O}_3$ , BCTZ, ceramics [3–6] have attracted great attention due to the excellent piezoelectric properties (with  $d_{33} = 500\text{--}600$  pC/N). Depending on the chemical composition,

various ferroelectric/antiferroelectric or paraelectric phases with slightly different dielectric properties and crystal structures of different type are formed. In all ferroelectrics, in general, the study of electrical conductivity is very important to realize the associated physical properties and nature of conductivity in these materials, and it is well known that the interior defects such as A-site vacancies, space charge electrons or oxygen vacancies have great influence on ferroelectric fatigue or ionic conductivity of the material [7–10]. Considering that the solid defects play a decisive role in all of these applications, we find that it is very important to gain a fundamental understanding of their conductive mechanism. Various kinds of defects are always suggested as being responsible for the dielectric relaxations at high temperature range. The AC impedance analysis is a powerful means to separate out the grain boundary and grain effects, which are usually the sites of trap for defects. It is also useful to establish its relaxation mechanism by appropriately assigning different values of resistance and capacitance to the grain and grain boundary effects. In

\* Corresponding author: tel: +213 26 21 56 51  
fax: +213 26 21 29 68, e-mail: [ahchaouchi@yahoo.fr](mailto:ahchaouchi@yahoo.fr)

this paper, a detailed analysis by AC impedance spectroscopy and dielectric relaxation has been carried out to characterize the dielectric and conductivity properties of  $(\text{Ba}_{0.85}\text{Ca}_{0.15})(\text{Ti}_{0.9}\text{Zr}_{0.1})\text{O}_3$  in order to gain insight into the relaxation mechanism and defects relation.

## II. Background

The AC Impedance is a non-destructive experimental technique for the characterization of microstructural and electrical properties of many electronic materials [11]. The technique is based on analysing the AC response of a system to a sinusoidal perturbation and subsequent calculation of impedance as a function of the frequency of the perturbation. The analysis of the electrical properties (conductivity, dielectric constant, loss, etc.) carried out using relaxation frequency ( $\omega_{max}$ ) values gives unambiguous results when compared with those obtained at arbitrarily selected fixed frequencies. The frequency dependent properties of a material can be described as complex permittivity ( $\epsilon^*$ ), complex impedance ( $Z^*$ ), complex admittance ( $Y^*$ ), complex electric modulus ( $M^*$ ) and dielectric loss or dissipation factor ( $\text{tg}\delta$ ). The real ( $\epsilon'$ ,  $Z'$ ,  $Y'$ ,  $M'$ ) and imaginary ( $\epsilon''$ ,  $Z''$ ,  $Y''$ ,  $M''$ ) parts of the complex parameters are in turn related to one another as follows:

$$\epsilon^* = \epsilon' + j \epsilon'' \quad (1)$$

$$Z^* = Z' + j Z'' = (1 / j C_0 \epsilon^* \omega) \quad (2)$$

$$Y^* = Y' + j Y'' = j \omega C_0 \epsilon^* \quad (3)$$

$$M^* = M' + j M'' = (1 / \epsilon^*) = j \omega \epsilon_0 Z^* \quad (4)$$

$$\text{tg}\delta = \epsilon'' / \epsilon' = M'' / M' = Y'' / Y' = Z'' / Z' \quad (5)$$

where  $\omega = 2\pi f$  is the angular frequency,  $C_0$  is the free geometrical capacitance, and  $j^2 = -1$ . These relations offer wide scope for a graphical analysis of the various parameters under different conditions of temperature or frequency. The useful separation of intergranular phenomena depends ultimately on the choice of an appropriate equivalent circuit to represent the sample properties.

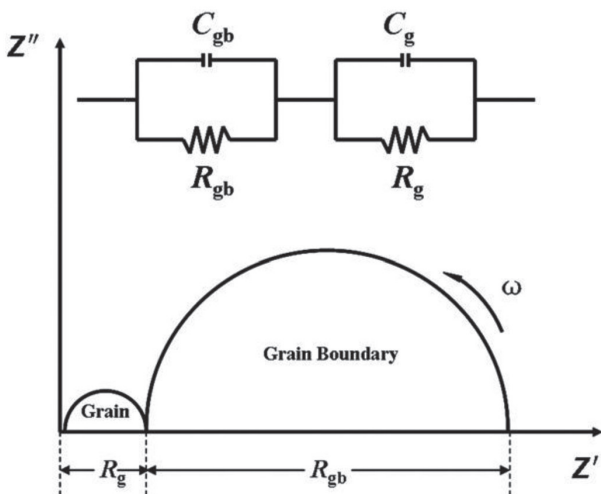


Figure 1. Electrical model of equivalent circuit and its Cole-Cole plot

From the microstructural point of view, a ceramic sample was composed of grains and grain boundaries, which had different resistivity ( $\rho$ ) and dielectric permittivity ( $\epsilon$ ) [12]. The electrical model of equivalent circuit is shown in the inset of Fig. 1. The real part ( $Z'$ ) and imaginary part ( $Z''$ ) of the complex impedance are given below [13]:

$$Z' = R_g / (1 + (\omega R_g C_g)^2) + R_{gb} / (1 + (\omega R_{gb} C_{gb})^2) \quad (6)$$

$$Z'' = \omega R_g^2 C_g / (1 + (\omega R_g C_g)^2) + \omega R_{gb}^2 C_{gb} / (1 + (\omega R_{gb} C_{gb})^2) \quad (7)$$

where  $R_g$  and  $C_g$  are the resistance and capacitance of the grain, while  $R_{gb}$  and  $C_{gb}$  are the resistance and capacitance of the grain boundary, respectively.

## III. Experimental

$(\text{Ba}_{0.85}\text{Ca}_{0.15})(\text{Ti}_{0.9}\text{Zr}_{0.1})\text{O}_3$  (BCTZ) ceramic powder was prepared by solid state reaction route. In this synthesis method, barium carbonate ( $\text{BaCO}_3$ ) (99.9%), titanium oxide ( $\text{TiO}_2$ ) (99.9%), zirconium oxide ( $\text{ZrO}_2$ ) (99.9%) and calcium carbonate ( $\text{CaCO}_3$ ) (99.9%) are used as raw materials. These compounds were stoichiometrically mixed using ethanol and zircon balls in a teflon jar for 2 hours. The slurry was subsequently dried and the powder was manually reground and heat treated at 1350 °C for 2 hours in air. The powder was finally reground using the same process in ethanol solution for 2 hours.

To manufacture pellets, an organic binder (polyvinyl alcohol, 5 vol.%) was manually added to the powder and disks (7 and 13 mm in diameter, 1.5 mm and 1 mm thickness, respectively) were shaped by uni-axial pressing under 100 MPa. The green samples were finally sintered in air at 1500 °C for 2 hours, with heating and cooling rates of 150 °C/h. The crystallised phase composition is identified by X-ray diffraction (XRD) technique using the  $\text{Cu K}\alpha$  X-ray radiation (Philips X' Pert) and the microstructures were observed using a scanning electron microscopy (SEM Philips XL'30). The specimens were polished and then coated with a silver paste. The dielectric and electric properties were determined using HP4284A meter versus temperature (from 20 °C to 600 °C) in the frequency range from 100 KHz to 1 MHz.

## IV. Results and discussion

### 4.1 Phase analysis and microstructure

The XRD pattern (Fig. 2) shows that the ceramics sintered at 1500 °C for 2 h present a single phase perovskite structure. Moreover, the presence of sharp and well-defined diffraction peaks indicate that this ceramic material has a degree of crystallinity at a long range, and without the presence of secondary phase containing Zr. These results suggest that  $\text{Ca}^{2+}$  and  $\text{Zr}^{4+}$  have been successfully incorporated into  $\text{BaTiO}_3$  lattice to form a homogeneous solid solution.

Figure 3 shows a typical SEM micrograph of the BCTZ ceramics. As can be seen in this micrograph, the

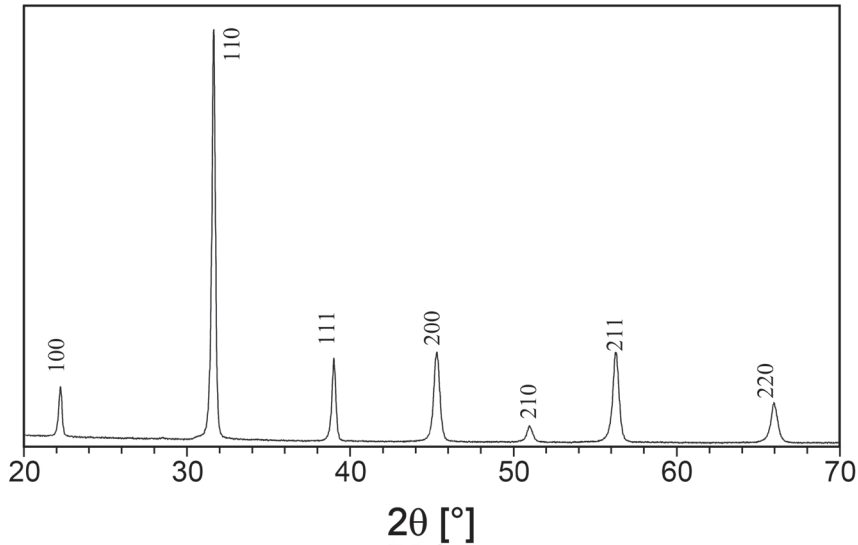


Figure 2. X-ray diffraction patterns of  $(\text{Ba}_{0.85}\text{Ca}_{0.15})(\text{Ti}_{0.9}\text{Zr}_{0.1})\text{O}_3$  sample sintered at 1500 °C for 2 hours

BCTZ ceramics is composed of large grains with an average size of approximately 30  $\mu\text{m}$ . We believe that these morphological characteristics are governed by the matter transport mechanism between the grains during the sintering process.

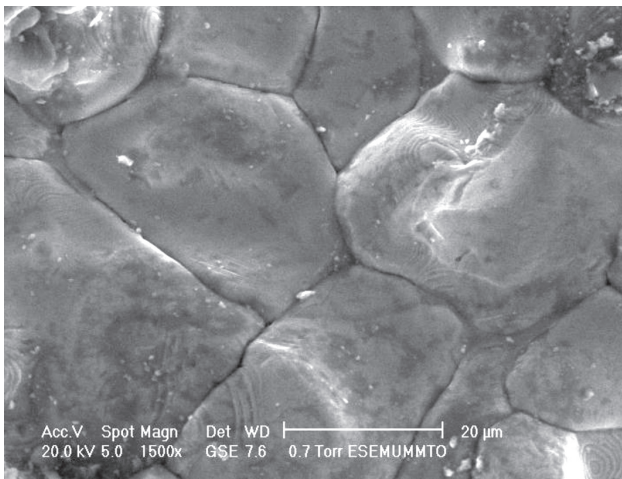


Figure 3. Scanning electron micrographs of fracture for the ceramics sintered at 1500 °C for 2 hours

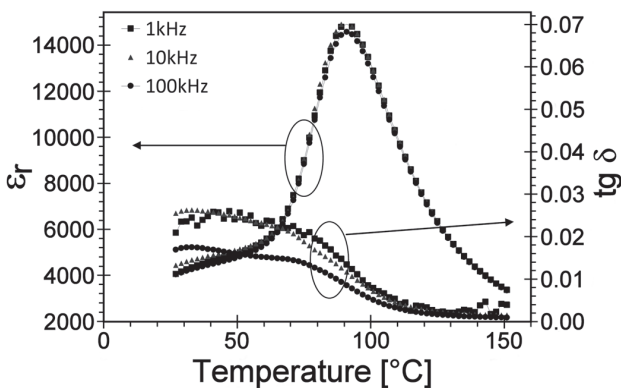


Figure 4. Temperature dependence of permittivity and dielectric loss at different frequency of  $(\text{Ba}_{0.85}\text{Ca}_{0.15})(\text{Ti}_{0.9}\text{Zr}_{0.1})\text{O}_3$  ceramics

#### 4.2 Dielectrics proprieties

Figure 4 exhibits the temperature dependence of dielectric constant and dielectric loss of the BCTZ ceramics at different frequencies. As it can be seen, the peak at 90 °C is observed on the dielectric constant versus temperature curves which corresponds to the phase transition of tetragonal phase to cubic one. It is also observed that the compound has the same  $T_c$  at all the above-mentioned frequencies indicating that it does not show relaxor behaviour. The good dielectric properties are obtained: important ambient dielectric constant ( $\epsilon_r = 4500$ ) with low dielectric losses  $\text{tg}\delta < 0.02$ .

#### 4.3 Impedance studies

Figure 5 show the variation of the real part of impedance ( $Z'$ ) with frequency at various temperatures. It is observed that the magnitude of  $Z'$  decreases with the increase in frequency for different measured temperature. The  $Z'$  values for all temperatures merge above 100 kHz. This may be due to the release of space charges as a result of reduction in the barrier properties of material with the rise in temperature and may be

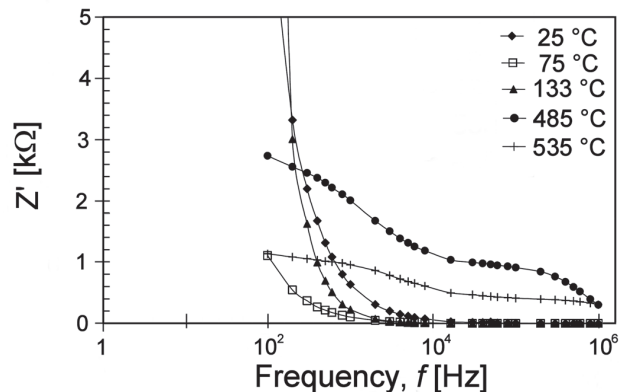


Figure 5. Variation of real part of impedance ( $Z'$ ) of  $(\text{Ba}_{0.85}\text{Ca}_{0.15})(\text{Ti}_{0.9}\text{Zr}_{0.1})\text{O}_3$  with frequency at different temperature

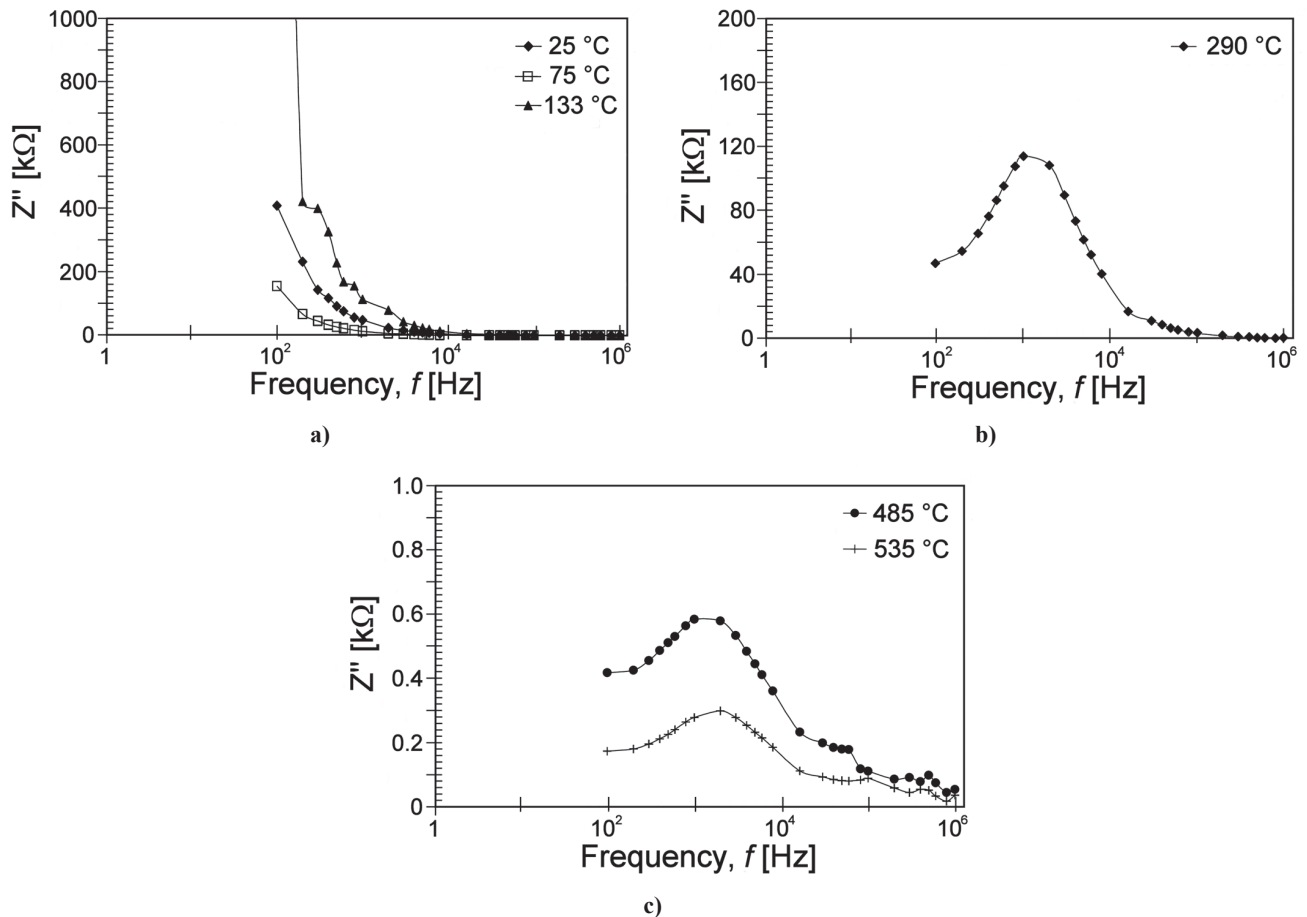


Figure 6. Variation of imaginary part ( $Z''$ ) of impedance of  $(\text{Ba}_{0.85}\text{Ca}_{0.15})(\text{Ti}_{0.9}\text{Zr}_{0.1})\text{O}_3$  with frequency at different temperatures: a) 25, 75 and 133 °C, b) 290 °C and c) 485 and 535 °C

a responsible factor for the enhancement of AC conductivity of material with temperature at higher frequencies. Further, at low frequencies the  $Z'$  values decrease with the rise in temperature, i.e. show negative temperature coefficient of resistance (NTCR) behaviour similar to semiconductors.

Figure 6 shows the variation of the imaginary part of impedance ( $Z''$ ) with frequency at different temperatures. The curves show that the  $Z''$  values reach a maxima peak  $Z''_{\text{max}}$  for the temperatures  $\geq 290$  °C and the value of  $Z''_{\text{max}}$  shifts to higher frequencies with increasing temperature. The merging of  $Z''$  values in the high frequency region may possibly be an indication of the accumulation of space charges in the material. For the temperature below 133 °C, the peak was beyond the range of frequency measurement.

Furthermore, as evident from the plots, as the temperature increases the magnitude of  $Z''$  decreases, the effect being more pronounced at the peak position. The shift of the peak towards higher frequencies with the rise of the temperature indicates that more than one relaxation phenomena are present in our sample. The asymmetric peaks suggest the presence of electrical processes in the material with the spread of relaxation time, i.e. the existence of a temperature dependent electrical relaxation phenomenon in the material [14].

Figure 7 shows a set of impedance data taken over a wide frequency range at several temperatures as a Cole-Cole (Nyquist) diagram (complex impedance spectrum). It is observed that with the increase in temperature the slope of the lines decreases and the curve moves towards real ( $Z'$ ) axis indicating the increase in conductivity of the sample. At the temperature of 485 °C onwards two semicircles could be obtained with different values of resistance for grain ( $R_g$ ) and grain boundary ( $R_{gb}$ ). Hence grain and grain boundary effects could be separated at these temperatures. At 535 °C (Fig. 7), data show only grain boundary effect.

The semicircular pattern in the impedance spectrum is a representative of the electrical processes taking place in the material which can be expressed as an equivalent electrical circuit comprising of a parallel combination of resistive and capacitive elements. The presence of two semicircular arcs accordingly can be thought of as resulting from cascading effect of parallel combination of resistive and capacitive elements arising from the contribution of bulk property of the material and grain boundary effect. The high frequency semicircle is attributed to the bulk property of the material (parallel combination of bulk resistance and bulk capacitance), and low frequency semicircle is due to the grain boundary effects in the material (parallel combi-

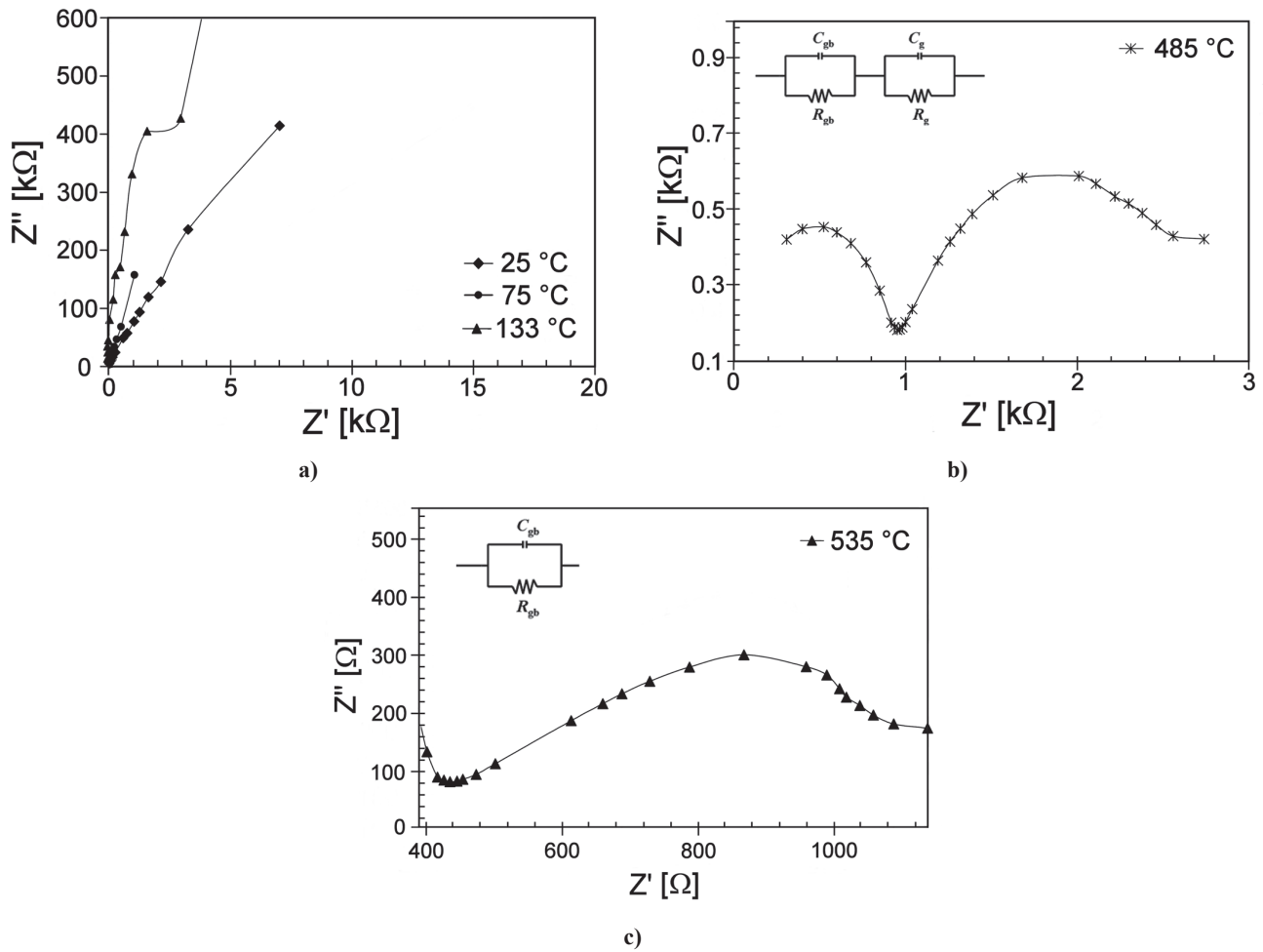


Figure 7. Complex impedance plots ( $Z''$  vs.  $Z'$ ) of  $(\text{Ba}_{0.85}\text{Ca}_{0.15})(\text{Ti}_{0.9}\text{Zr}_{0.1})\text{O}_3$  at different temperatures: a) 25, 75 and 133 °C, b) 485 °C and c) 535 °C. Inset shows the appropriate equivalent electrical circuit.

nation of grain boundary resistance and capacitance). The electrical processes taking place within the material has been modelled for a polycrystalline system and is shown in terms of the equivalent electrical circuit in the Fig. 7 (inset).

Modulus analysis is an alternative approach to explore electrical properties of the material and magnify any other effects present in the sample as a result of dif-

ferent relaxation time constants. The values of real ( $M'$ ) and imaginary ( $M''$ ) components of the modulus are obtained from the following expressions:

$$M' = \omega C_0 Z' \tag{8}$$

$$M'' = \omega C_0 Z'' \tag{9}$$

where  $C_0$  is the geometrical capacitance of the empty cell.

Figure 8 shows the variation of  $M''$  as a function of frequency. It exhibits that the maxima of the imaginary component of modulus ( $M''_{max}$ ) shifts towards higher relaxation frequency with rise in temperature. This behaviour suggests that the dielectric relaxation is thermally activated in which hopping mechanism of charge carriers dominates intrinsically [15]. The asymmetric broadening of the peak indicates the spread of relaxation with different time constant, and hence the relaxation in the material is of non-Debye type.

The scaling behaviour of the sample was studied by plotting normalized parameters (i.e.  $M''/M''_{max}$  versus  $\log(f/f_{max})$ , where  $f_{max}$  is frequency corresponding to  $M''_{max}$ ) at different measuring temperatures and is shown in Fig. 9. The modulus scaling behaviour gives an insight into the dielectric processes occurring inside the material [16]. The low frequency side of the peak in

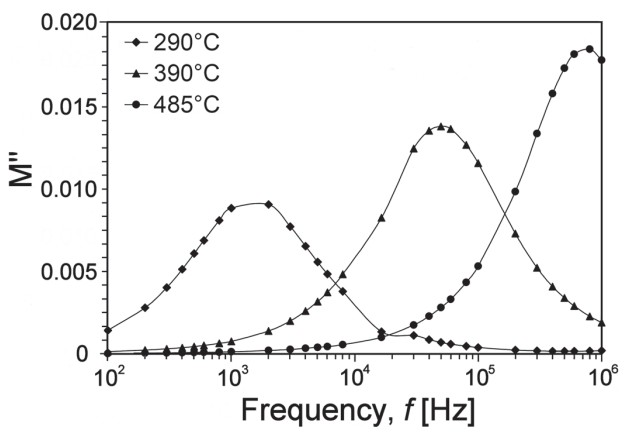


Figure 8. Variation of imaginary part of modulus ( $M''$ ) with frequency

$M''/M''_{max}$  versus  $\log(f/f_{max})$  curve represents the range of frequencies in which the charge carriers can cover a longer distance by successfully hopping from one site to another site. The high frequency side of  $M''/M''_{max}$  versus  $\log(f/f_{max})$  curve represents the range of frequencies in which the charge carriers are spatially confined to their potential wells, and therefore can make only localized motions inside the well.

The region where the peak occurs is an indication of the transition from the long-range to the short-range

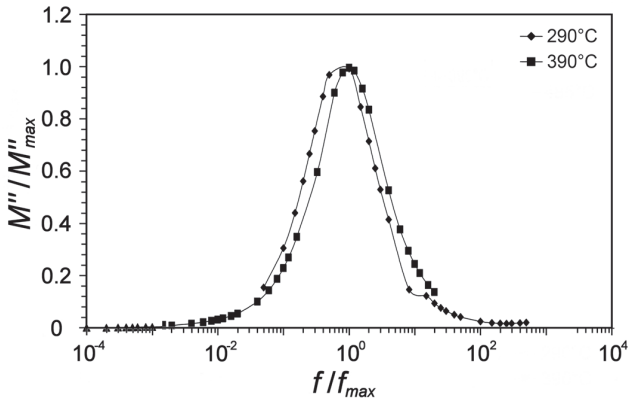


Figure 9. Modulus scaling behaviour ( $M''/M''_{max}$ ) versus  $\log(f/f_{max})$

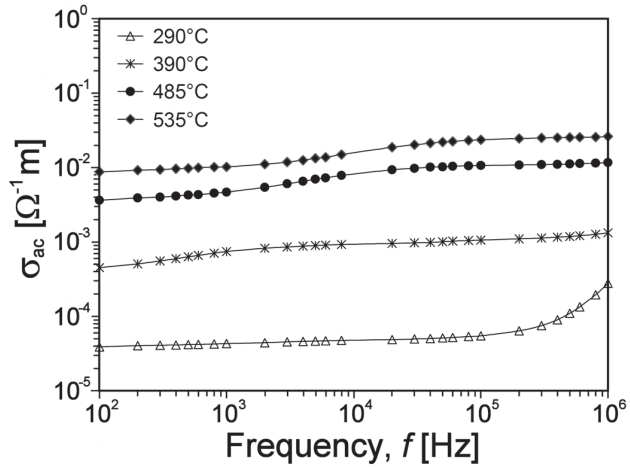


Figure 10. Frequency dependence of AC conductivity at different temperatures

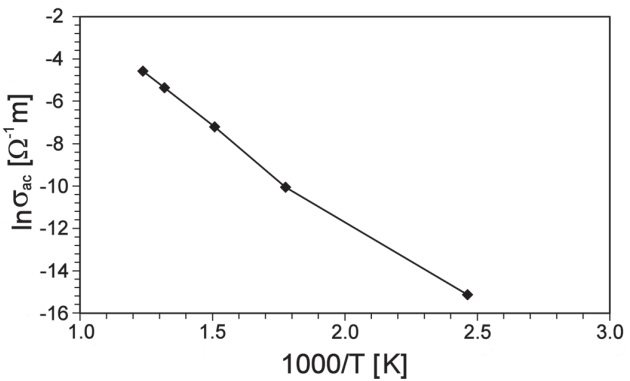


Figure 11. Variation of ac conductivity with inverse absolute temperature at 1kHz

mobility with the increase in frequency [16]. The overlapping of all the curves/peaks of different temperatures indicates temperature independent behaviour of the dynamic processes occurring in the material [17].

The AC (bulk) conductivity,  $\sigma_{ac}$  of the sample has been evaluated from the impedance spectrum using the relation:

$$\sigma_{ac} = t / R_b A \tag{10}$$

where  $R_b$  is the bulk resistance,  $t$  the thickness, and  $A$  the surface area of the sample.

Variation of AC conductivity with frequency at various temperatures can be understood from Fig. 10 where at lower frequencies plateaus of  $\sigma_{ac}$  (i.e. frequency independent values of conductivity) corresponds to the dc conductivity. The frequency dependent conductivity can be described by the equation:

$$\sigma_{ac}(\omega) = \sigma_{dc} + A\omega^n \tag{11}$$

where  $n$  is the frequency exponent in the range of  $0 < n < 1$ .  $A$  and  $n$  are thermally activated quantities, hence electrical conduction is a thermally activated process. According to Jonscher [18], the origin of the frequency dependence of conductivity lies in the relaxation phenomena arising from mobile charge carriers. When mobile charge carriers hop into a new site from its original position, it remains in a state of displacement between two potential energy minima, which includes contributions from other mobile defects after sufficient time. The defect could relax until the two minima in lattice potential energy coincide with the lattice site.

Figure 11 shows the variation of  $\ln \sigma_{ac}$  with  $10^3/T$ . It is observed that  $\sigma_{ac}$  increase with increasing temperature further confirming the NTCR behaviour. The nature of variation is linear and follows the Arrhenius relationship:

$$\sigma_{ac} = \sigma_0 \exp(-E_a/k_B T) \tag{12}$$

where  $E_a$  is the activation energy of conduction and  $T$  is the absolute temperature. The value of activation energy ( $E_a$ ) as calculated from the slope of  $\ln \sigma_{ac}$  with  $10^3/T$  curve is found to be 0.7433 eV, which suggests that the conduction may be the result of defect and associated charge carriers of metals ions [19].

### V. Conclusions

Polycrystalline  $(Ba_{0.85}Ca_{0.15})(Ti_{0.9}Zr_{0.1})O_3$ , prepared through a high-temperature solid-state reaction technique, was found to have a single-phase perovskite-type structure. Impedance analyses indicated the presence of grain and grain boundary effects in (BCTZ) ceramics. Sample showed dielectric relaxation which is found to be of non-Debye type and the relaxation frequency shifted to higher side with the increase of temperature. The The Cole-Cole (Nyquist) plot and conductivity studies showed the NTCR character of BCTZ. The

frequency dependent AC conductivity at different temperatures indicated that the conduction process is thermally activated process. The value of activation energy ( $E_a$ ) as calculated from the slope of  $\ln\sigma_{ac}$  with  $10^3/T$  curve is found to be 0.7433 eV, which suggests that the conduction may be the result of defect and associated charge carriers of metals ions.

## References

1. J.F. Tressler, S. Alkroy, R.E. Newnham, "Piezoelectric sensors and sensor materials", *J. Electroceram.*, **2** (1998) 257–272.
2. European Union, Restriction of Hazardous substances (RoHS), Directive 2002/95/EC; and 2008/34/EC on Waste Electrical and Electronic Equipment (WEEE).
3. W. Li, Z. Xu, R. Chu, P. Fu, G. Zang, "Piezoelectric and dielectric properties of  $(\text{Ba}_{1-x}\text{Ca}_x)(\text{Ti}_{0.95}\text{Zr}_{0.05})\text{O}_3$  lead-free ceramics", *J. Am. Ceram. Soc.*, **93** [10] (2010) 2942–2944.
4. M. Porta, T. Lookman, A. Saxena, "Effects of criticality and disorder on piezoelectric properties of ferroelectrics", *J. Phys.: Condensed Matter*, **22** [34] (2010) 345902.
5. W. Li, Z. Xu, R. Chu, P. Fu, G. Zang, "High piezoelectric  $d_{33}$  coefficient in  $(\text{Ba}_{1-x}\text{Ca}_x)(\text{Ti}_{0.98}\text{Zr}_{0.02})\text{O}_3$  lead-free ceramics with relative high Curie temperature", *Mater. Lett.*, **64** [21] (2010) 2325–2327.
6. W. Li, Z. Xu, R. Chu, P. Fu, G. Zang, "Polymorphic phase transition and piezoelectric properties of  $(\text{Ba}_{1-x}\text{Ca}_x)(\text{Ti}_{0.9}\text{Zr}_{0.1})\text{O}_3$  lead-free ceramics", *Phys. B: Condensed Matter*, **405** [21] (2010) 4513–4516.
7. K. Goda, M. Kuwabara, *Ceram. Trans.*, **22** (1991) 503.
8. M. Kchikech, M. Belkaoumi, M. Maglione, "Space-charge relaxation in perovskites", *Phys. Rev. B*, **49** (1994) 7868–7873.
9. A.P. Li, X.U. Chen, J.S. Lu, X. Zhu, "Collective domain-wall pinning of oxygen vacancies in bismuth titanate ceramics", *J. Appl. Phys.*, **98** (2005) 024109.
10. Z.A. Yu, L.E. Cross, "Oxygen-vacancy-related low frequency dielectric relaxation and electrical conduction in  $\text{Bi:SrTiO}_3$ ", *Phys. Rev. B*, **62** (2000) 228–236.
11. J.R. Macdonald, *Impedance Spectroscopy*, Wiley, New York, 1987.
12. J.R. Dygas, G. Fafilek, M.W. Breiter, "Study of grain boundary polarization by two-probe and four-probe impedance spectroscopy", *Solid State Ionics*, **119** (1999) 115–125.
13. H.T. Langhammer, D. Makovec, Y. Pu, H.-P. Abicht, M. Drofenik, "Grain boundary reoxidation of donor-doped barium titanate ceramics", *J. Eur. Ceram. Soc.*, **26** (2006) 2899–2907.
14. C.K. Suman, K. Prasad, R.N.P. Choudhary, "Impedance spectroscopic studies of ferroelectric  $\text{Pb}_2\text{Sb}_3\text{DyTi}_5\text{O}_{18}$  ceramic", *Adv. Appl. Ceram.*, **104** (2005) 294–299.
15. B. Behera, P. Nayak, R.N.P. Choudhary, "Structural and impedance properties of  $\text{KBa}_2\text{V}_5\text{O}_{15}$  ceramics", *Mater. Res. Bull.*, **43** (2008) 401–410.
16. P.S. Das, P.K. Chakraborty, B. Behera, R.N.P. Choudhary, "Electrical properties of  $\text{Li}_2\text{BiV}_5\text{O}_{15}$  ceramics", *Physica B*, **395** (2007) 98–103.
17. S. Saha, T.P. Sinha, "Low-temperature scaling behavior of  $\text{BaFe}_{0.5}\text{Nb}_{0.5}\text{O}_3$ ", *Phys. Rev. B*, **65** (2002) 134103.
18. A.K. Jonscher, "The 'universal' dielectric response", *Nature*, **267** (1977) 673–679.
19. A. Hussain, C.W. Ahn, H.J. Lee, I.W. Kim, J.S. Lee, S.J. Jeong, S.K. Rout, "Anisotropic electrical properties of  $\text{Bi}_{0.5}(\text{Na}_{0.75}\text{K}_{0.25})_{0.5}\text{TiO}_3$  ceramics fabricated by reactive templated grain growth (RTGG)", *Curr. Appl. Phys.*, **10** (2010) 305–310.

